ACS APPLIED MATERIALS & INTERFACES

Research Article

www.acsami.org

Carboxybetaine Methacrylate-Modified Nylon Surface for Circulating Tumor Cell Capture

Huiyu Wang,[†] Guofeng Yue,[‡] Chaoqun Dong,[§] Fenglei Wu,[†] Jia Wei,[∥] Yang Yang,[∥] Zhengyun Zou,[∥] Lifeng Wang,[∥] Xiaoping Qian,[∥] Tao Zhang,*[,§] and Baorui Liu*[,†]

[†]Nanjing Drum Tower Hospital, Clinical College of Nanjing Medical University, 321 Zhongshan Road, Nanjing 210008, China

[‡]Nanjing Medical University, 140 Hanzhong Road, Nanjing 210029, China

[§]College of Engineering and Applied Sciences, Nanjing University, 22 Hankou Road, Nanjing 210093, China

[∥]The Comprehensive Cancer Centre of Drum Tower Hospital, Medical School of Nanjing University, Clinical Cancer Institute of Nanjing University, 321 Zhongshan Road, Nanjing 210008, China

Supporting Information

ABSTRACT: Conventional *in vitro* circulating tumor cell (CTC) detection methods are always limited by blood sample volume because of the requirement of a large amount of blood. The aim of this study was to overcome the limitation by designing and making an *in vivo* CTC capture device. In this study, we designed and prepared a kind of proper material to serve the purpose of intervention. A method employing 3-aminopropyltriethoxysilane (γ-APS) as the coupling reagent to graft carboxybetaine methacrylate (CBMA) and to immobilize an anti-epithelial cell adhesion molecular (EpCAM) antibody on Nylon was developed. The results of X-ray photoelectron spectroscopy and Fourier transform infrared spectroscopy proved the successful graft of γ-APS and CBMA to Nylon. Furthermore, the predicted improvement in the biocompatibilities of our modified Nylon was confirmed by water contact angle measurement, bovine serum albumin adhesion, platelet adhesion, plasma recalcification time determination, and cytotoxicity tests. The tumor cells adhesion experiment revealed that Nylon with the antibody immobilized on it had an affinity for EpCAM positive tumor cells higher than that of pristine Nylon. Additionally, the capture ability of the CTCs was demonstrated in a nude mouse tumor model using the interventional device made of the modified Nylon wire. The positive results suggest that CBMA-grafted and anti-EpCAM antibody-immobilized Nylon is a promising new material for *in vivo* CTC capture devices.

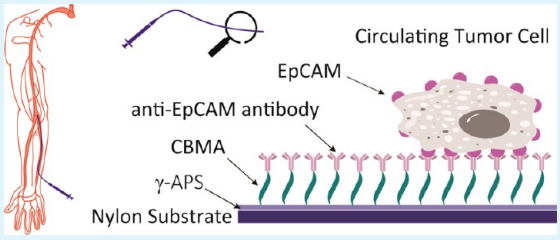

KEYWORDS: *surface modification, Nylon, carboxybetaine methacrylate, circulating tumor cells, interventional device*

1. INTRODUCTION

The so-called circulating tumor cells (CTCs) are tumor cells that are shed from the primary site flowing in the bloodstream. The transportation of CTCs to distant organs that will lead to the formation of metastasis remains the major cause of cancer-related death.[1] Recent studies demonstrated the prognostic importance of CTC detection in patients with lung cancer,[2] breast cancer,[3−5] colorectal cancer,[6] melanoma,[7] and prostate cancer.[8] The molecular analysis of CTCs promoted the development of a new concept, "liquid biopsy", which allows personalized selections of anticancer drugs.[9] Given its great value in the clinical management of cancer patients, the detection of CTCs becomes one of the hottest research topics. Extensive studies in this field have led to rapid developments of various detection methods.[10−22] Recently, surface modification has been widely adopted to make functional devices for CTC capture.[23−27] For instance, Wang and colleagues developed gold nanoparticle layers with different roughnesses modified with poly[oligo(ethylene glycol) methacrylate] and TD05 aptamer to capture RAMOS cells in a serum environment.[23] Also, Sokolov's team attached antibodies to the gold shell/magnetic core nanoparticles via a heterofunctional PEG linker during the fabrication of their CTC capture device.[24] Despite all the progress that has been made, the detection of CTCs remains a technical challenge because as few as one CTC exists in a background of up to 10^8 normal blood cells.[28] Traditional *in vitro* CTC detection methods that work by capturing tumor cells in blood samples require ∼7.5 mL of blood in total to be drawn from cancer patients. The need for a large amount of blood limits the application of traditional *in vitro* CTC detection methods. This study aims to overcome this limitation. We designed an interventional device that may catch more CTCs by remaining in the vein for a period of time and thereby contact a larger volume of blood. In this study, we focused on the preparation of the proper material that is needed for the future manufacture of the *in vivo* CTC capture device.

Nylon has been widely used as a biomaterial because of its outstanding physicochemical properties.[29−31] However, Nylon

Received: January 19, 2014
Accepted: February 26, 2014
Published: February 26, 2014

   dx.doi.org/10.1021/am500394j | ACS Appl. Mater. Interfaces 2014, 6, 4550−4559

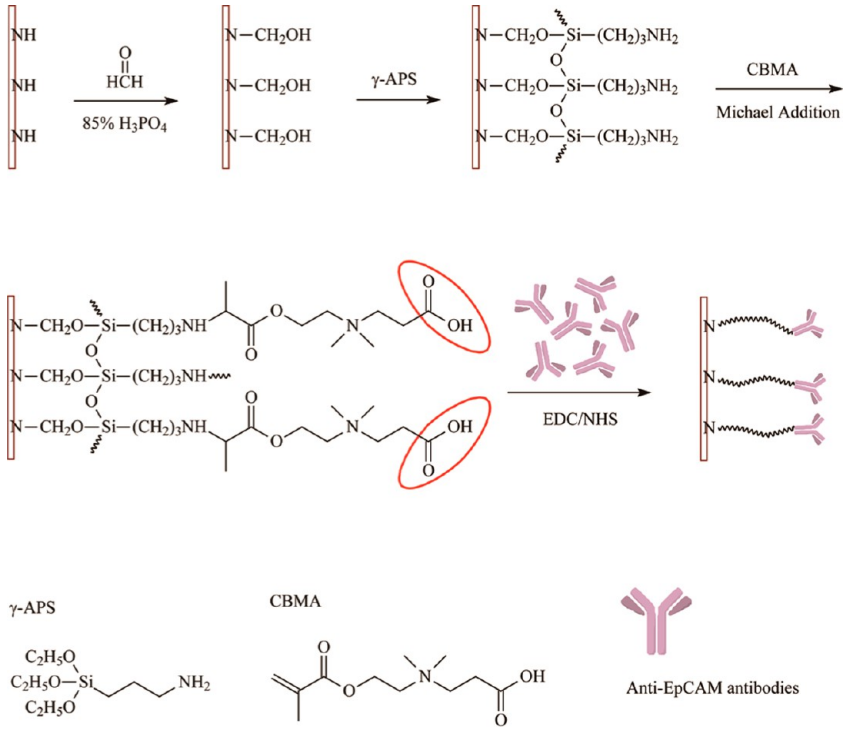

Figure 1. Preparation of the CBMA-grafted and antibody-immobilized Nylon surface.

is a kind of relatively inert polymer. A novel and convenient method for modifying a Nylon surface to obtain better biocompatibility and immobilizing antibodies to CTCs is necessary.

Carboxybetaine methacrylate (CBMA) is a zwitterionic compound that has a structure similar to that of glycine betaine, which is vital for the osmotic regulation of body fluid.[32] It is known that CBMA has extremely good blood compatibility and that CBMA is an ideal material for biomedical applications.[33−36] Moreover, antibodies can be covalently linked to CBMA by 1-ethyl-3-[3-(dimethylamino)propyl]-carbodiimide and *N*-hydroxysuccinimide (EDC/NHS) chemistry that involves the carboxylic groups of CBMA and the amino groups of antibodies.

We developed a method that employs 3-aminopropyltriethoxysilane (γ-APS) as a coupling reagent to graft CBMA and the anti-EpCAM antibody to the Nylon surface to improve Nylon's biocompatibility, therefore making Nylon qualified for capturing CTCs *in vivo*. X-ray photoelectron spectroscopy (XPS) and Fourier transform infrared spectroscopy (FTIR) experiments were performed to confirm the graft. The improvement in blood compatibility of CBMA-grafted Nylon was demonstrated by water contact angle measurement, bovine serum albumin (BSA) adhesion, platelet adhesion, and plasma recalcification time determinations. No obvious cytotoxicity was found in cytotoxicity tests of CBMA-grafted Nylon. We found that a CBMA-grafted and antibody-immobilized Nylon surface can conglutinate more EpCAM positive tumor cells than pristine Nylon in a tumor cell adhesion experiment. Moreover, the nude mouse tumor model was employed to demonstrate the ability of the modified Nylon to capture CTCs *in vivo*. These results suggest that Nylon modified by our method is a suitable and promising material for the interventional CTC detection device.

2. EXPERIMENTAL SECTION

2.1. Materials and Reagents. 2-(*N*,*N*′-Dimethylamino)ethyl methacrylate (DMAEM, 98%), 3-chloropropionic acid, 3-aminopropyltriethoxysilane (γ-APS), and 4-methoxyphenol (MEHQ) were purchased from Aladdin-Reagent Co. Ltd. (Shanghai, China). Rabbit anti-human EpCAM monoclonal IgG and the anti-pan Cytokeratin antibody (FITC) were purchased from abcam (catalog nos. ab32392 and ab78478, respectively). HRP-conjugated goat anti-rabbit IgG and 3,3′-diaminobenzidine chromogen were purchased from Boster Co. Ltd. (Wuhan, China). Hematoxylin, 4′,6-diamidino-2-phenylindole (DAPI), and BSA were supplied by the Beyotime Institute of Biotechnology (Jiangsu, China). BCA and the microBCA protein assay kit were purchased from Thermo Fisher Scientific Inc. (Rockford, IL). The 16 gauge medical trocar was a product of BD Co. Nylon-12 samples and wires were kindly provided by Freewell biotechnology Co. Ltd. (Nanjing, China).

2.2. Synthesis of CBMA. CBMA was synthesized by the reaction of DMAEM and sodium 3-chloropropionate (synthesized by neutral reaction of 3-chloropropionic acid and sodium hydroxide). DMAEM (15.7 g, 0.1 mol), sodium 3-chloropropionate (13.7 g, 0.105 mol), and MEHQ (0.03 g, 0.0002 mol) were mixed and stirred under nitrogen at 70 °C for ∼6 h. The obtained liquid was dropped into tetrahydrofuran, and the white precipitate was produced by suction filtration. Then, the white precipitate was washed with anhydrous acetone and anhydrous ether. The final CBMA product was dried under reduced pressure and stored at 4 °C. The yield was 51%. ^{1}H NMR (Figure S1, Supporting Information) was recorded by using deuterated water as the solvent:[37] ^{1}H NMR (300 MHz) δ 6.06 (s, 1H, =CH), 5.68 (s, 1H, =CH), 4.55 (t, 2H, OCH_2), 3.70 (t, 2H, CH_2N), 3.59 (t, 2H, NCH_2), 3.10 (s, 6H, NCH_3), 2.64 (t, 2H, CH_2COO), 1.84 (s, 3H, $=CCH_3$).

2.3. CBMA Graft and Antibody Immobilization. Surface modification was conducted on 10 mm × 10 mm × 3 mm Nylon pieces and 100 mm long Nylon wires. Before the modification, Nylon samples were ultrasonically cleaned in acetone and soaked in 10% sodium hydroxide for 1 h. Then, *N*-methylol polyamide (Nylon-OH) was produced as previously reported.[38] After Nylon-OH had been silanized with 3-aminopropyltriethoxysilane,[39] the CBMA graft was achieved by means of Michael addition.[40] Thereafter, EDC/NHS chemistry was introduced in the immobilization of antibodies.[41]

dx.doi.org/10.1021/am500394j | ACS Appl. Mater. Interfaces 2014, 6, 4550−4559

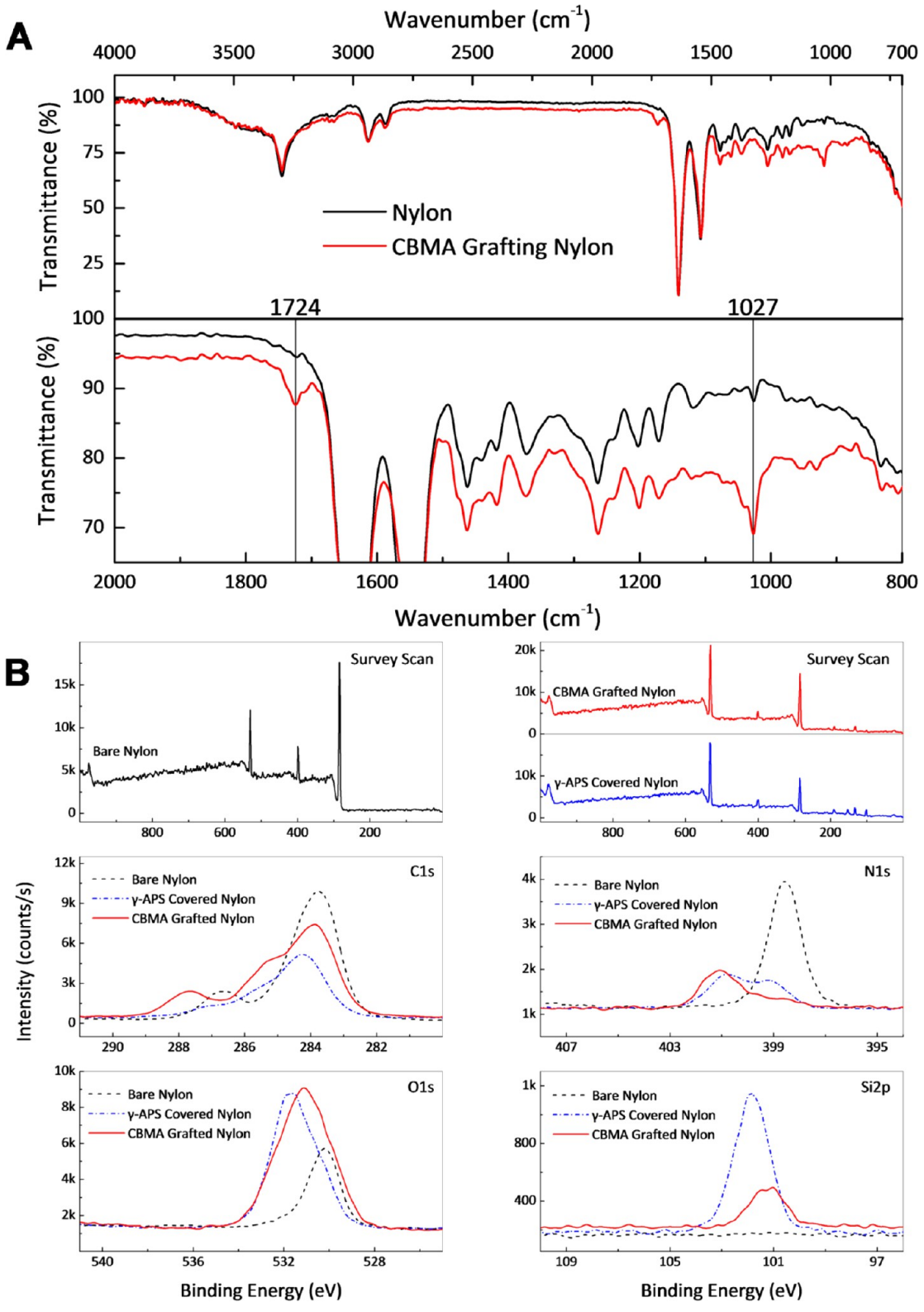

Figure 2. (A) ATR-FTIR and (B) XPS spectra of bare Nylon, γ-APS-covered Nylon, and CBMA-grafted Nylon surfaces. In graph A, the bottom panel is an enlarged part (from 800 to 2000 cm^{-1}) of the top panel.

Briefly, 85 wt % phosphoric acid (1 mL) and a formaldehyde solution (50 mL) were decanted to a flask containing Nylon samples and kept at 60 °C for 12 h to produce the hydroxyl groups on the Nylon surface. Nylon-OH samples were soaked in a 1 vol % anhydrous ethanol solution of γ-APS for 1 h at room temperature. After being rinsed with ethanol and dried at 60 °C for 2 h, the Nylon samples were soaked in a 2 wt % water solution of CBMA for 24 h. The samples were dried and kept at room temperature. The CBMA-grafted Nylon samples were activated before antibody immobilization by incubation in a dioxane/water [14:1 (v/v)] solution of EDC (2 mg/mL) and NHS (2 mg/mL) for 1 h at room temperature. A 50 μL drop of the PBS solution containing 100 μg/mL anti-EpCAM antibodies was put

on each Nylon sample. The Nylon samples were covered by glass slips and stored at 4 °C for 24 h in a humid environment. Unreacted NHS was removed by treating the pieces with 1 M ethanolamine (pH 8.5) for 10 min (Figure 1). Then, samples were gently washed three times with PBS to remove nonimmobilized antibodies.

2.4. Surface Chemical Characterization of the Modified Nylon. Attenuated total reflectance Fourier transform infrared spectra (ATR-FTIR) were acquired via a Fourier transform infrared spectrometer (Thermo Nicolet Nexus 870). For each spectrum, a resolution of 4 cm^{-1} was applied and 32 scans were taken.

X-ray photoelectron spectroscopy (XPS) was conducted with a PHI 5000 VersaProbe Photoelectron Spectrometer (Physical Electronics) equipped with a monochromatic Al Kα X-ray source to verify the surface elemental compositions. The XPS spectra were recorded at a detection angle of 90°.

2.5. Wettability. The water contact angle (WCA) of the samples was measured with a KSV CAM200 optical contact angle and surface tension meter system (KSV Instruments) at 20 °C at a relative humidity of 85%. Each result was an average of eight determinations.

2.6. Protein Adsorption. Both pristine Nylon pieces and CBMA-grafted Nylon pieces were soaked in PBS for 24 h at room temperature and then immersed in a PBS solution of BSA (1, 0.5, and 0.1 mg/mL) for 2 h. After that, each piece was gently washed three times with PBS. To elute the adsorbed BSA, samples were soaked in a water solution of 1 wt % sodium dodecyl sulfonate (SDS) and oscillated at 37 °C for 1 h. The BSA concentration of the elution was measured with BCA and the microBCA protein assay kit, and the amount of adsorbed BSA on each was calculated. Each final result was an average of five determinations.

2.7. Platelet Adhesion. Nylon pieces were immersed in PBS for 24 h at room temperature before being assessed. A drop of 20 μL apheresis platelets (supplied by the Jiangsu Province Blood Center at a density of 1×10^6 platelets/μL) was dripped onto the Nylon surface and kept for 30 min at 37 °C. After being gently washed three times with PBS, the Nylon pieces were fixed with 2.5 wt % glutaraldehyde for an additional 30 min. Thereafter, the Nylon pieces were dehydrated sequentially with an ethanol aqueous solution series at concentrations of 50, 60, 70, 80, 90, 95, and 100% (v/v) for 15 min in each solution. The samples were observed by field-emitted scanning electron microscopy (SEM) (S-3400N II, Hitachi). Six different areas were randomly chosen to be counted.

2.8. Plasma Recalcification Time (PRT) Determination. Plasma was isolated from 2 mL of sodium citrate-processed blood drawn from a healthy donor. Before the determination, Nylon pieces were immersed in PBS for 24 h at room temperature. Clean glass slides with and without silicon oil were used as controls; 50 μL of plasma was dropped onto each sample surface. After the samples had been incubated at 37 °C for 1 min, 50 μL of a $CaCl_2$ (0.025 M) solution was added to the plasma drop. The elapsed time of the fibrin clotting formation was recorded. Each result is an average of six parallel experiments.

2.9. Cytotoxicity Assay. To examine the potential cytotoxic effects of CBMA-grafted Nylon, we chose human umbilical vein endothelial cells (HUVECs) as objects to perform the cytotoxic assay. The wirelike copper sample and the CBMA-grafted Nylon sample were immersed in an ECM culture solution for 24 h (3 cm^2 of copper or Nylon surface and 9 cm^2 of Nylon surface area soaked in 3 mL of an ECM culture solution, respectively). HUVECs were cultured using these three solutions for 24 h and fixed with paraformaldehyde for 15 min. The morphology of HUVECs was observed under a fluorescence microscope (Axio Scope A1, Zeiss) after CFSE incubation. The viability of HUVECs was tested with a cell counting kit (CCK8 KIT, Dojindo).

2.10. Tumor Cell Adhesion Experiments. *2.10.1. Cell Line and Cell Culture.* Human gastric cancer cell lines SGC7901, MKN28, BGC823, and MKN45 were purchased from the Shanghai Institute of Cell Biology (Shanghai, China). Cells were propagated in RPMI-1640 medium (Gibco-Invitrogen, Carlsbad, CA) supplemented with 10% fetal bovine serum (FBS) (Gibco-Invitrogen) in a humidified atmosphere containing 5% CO_2 at 37 °C.

2.10.2. Immunocytochemistry. SGC7901, MKN28, BGC823, and MKN45 cells for immunocytochemistry staining were prepared with a cytocentrifuge. After being washed twice with PBS, cells were fixed with cold acetone for 10 min and incubated with 0.03% hydrogen peroxide in PBS for 20 min to block endogenous peroxidase. Then, cells were incubated overnight at 4 °C with the anti-EpCAM antibody (1:100). After being washed with PBS, cells were treated with HRP-conjugated goat anti-rabbit IgG (1:1000). Sequentially, immunostaining for EpCAM was visualized via 3,3′-diaminobenzidine chromogen with hematoxylin counterstaining.

2.10.3. Tumor Cell Adhesion. Antibody-immobilized and pristine Nylon pieces were placed in the wells of a 24-well plate (Corning). Tumor cells (10^6) were diluted with 2 mL of PBS and then added to the wells containing the Nylon samples. The supernatant was discarded after incubation for 30 min. Thereafter, Nylon samples were gently washed three times with PBS to eliminate the uncaught cells and immersed in cold acetone for 10 min to fix the cells adhering to the surface. Finally, the cells were imaged and counted (Image-Pro Plus version 6.0, Media Cybernetics) under a fluorescence microscope (Axio Scope A1, Zeiss) after DAPI incubation for 10 min.

2.11. *In Vivo* CTC Capture on a Nude Mouse Tumor Model. We established the nude mouse orthotopic tumor model of human gastric cancer cell line SGC7901. Before the *in vivo* CTC capture was conducted, we dissected the postcava of the mouse and punctured it using the trocar (Figure S3, Supporting Information). Then, the 100 mm long CBMA-grafted and anti-EpCAM antibody-immobilized Nylon wire was placed into the canula. The ~10 mm long front end (working length) of the modified Nylon wire stayed in the postcava of the mouse contacting the blood for CTC capture. After being exposed to the blood flow for 30 min, the inserted Nylon wire was pulled out and gently washed with PBS. The wire was immersed in cold acetone for 10 min to fix the cells adhering to the surface. After successive incubation with a solution of BSA, the anti-pan Cytokeratin antibody (FITC), and DAPI, the surface of the wire was observed under a fluorescence microscope. In parallel, *in vivo* CTC capture using an unmodified Nylon wire was conducted on another nude mouse with a tumor.

2.12. Statistical Analysis. Statistical analyses of data were conducted by one-way analysis of variance or a Student's *t* test. The data are listed as means ± the standard deviation, and *p* values of <0.05 were accepted as being statistically significant.

3. RESULTS AND DISCUSSION

3.1. Surface Characterization. *3.1.1. ATR-FTIR.* ATR-FTIR spectra of pristine Nylon and CBMA-grafted Nylon are shown in Figure 2A. The additional peak at 1724 cm^{-1} that appears in the spectrum of CBMA-grafted Nylon belongs to ester carbonyl groups observed from the band of the O−C═O stretch. The successful CBMA graft could be ascertained from the presence of this characteristic peak. Additionally, enhancement of the peak at 1027 cm^{-1} that belongs to the C−O−C stretch enhances our conclusion of formation of a CBMA graft. Both Nylon and CBMA possess the C−O−C stretch; this peak can be observed in the spectrum of pristine Nylon. In the spectrum of CBMA-grafted Nylon, the enhancement of this peak reveals the increase in the amount of the C−O−C stretch and in turn proves the successful graft of CBMA.

3.1.2. XPS. The chemical composition of the sample surfaces can be conveniently investigated by XPS with high sensitivity. Figure 2B shows the overall and typical element spectra of pristine Nylon, γ-APS-modified Nylon, and CBMA-grafted Nylon surfaces. Three different types of carbon can be seen on the CBMA-grafted Nylon surface in the C1s spectrum. The three carbon types are the alkyl carbon of the −C−C*−C stretch with a binding energy of 283.8 eV, the ammonium carbon of the −N−C*− stretch at 286.8 eV, and the ester carbon of the −C*OO− group at 287.8 eV. Changes in peak

dx.doi.org/10.1021/am500394j | ACS Appl. Mater. Interfaces 2014, 6, 4550−4559

A

Substrate	Water contact angle (°)
Pristine nylon	75.05±0.77
CBMA grafted nylon	50.07±1.17

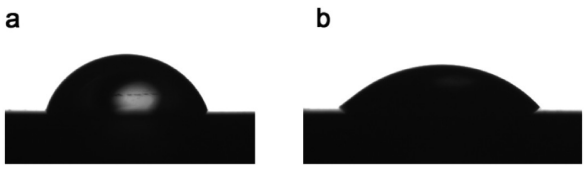

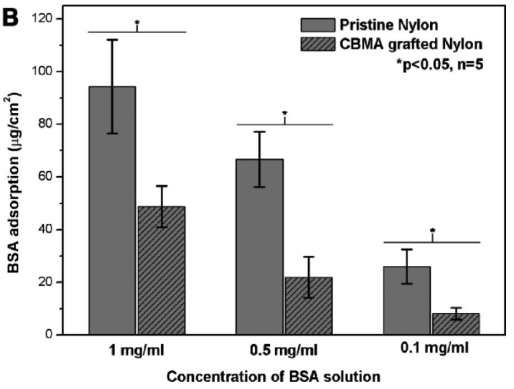

Figure 3. Results of water contact angle determination (A) and amounts of BSA adsorption (B) on pristine and CBMA-grafted Nylon surfaces. Panel A also shows the typical pictures of the water contact angle of Nylon surface before (a) and after (b) CBMA grafting.

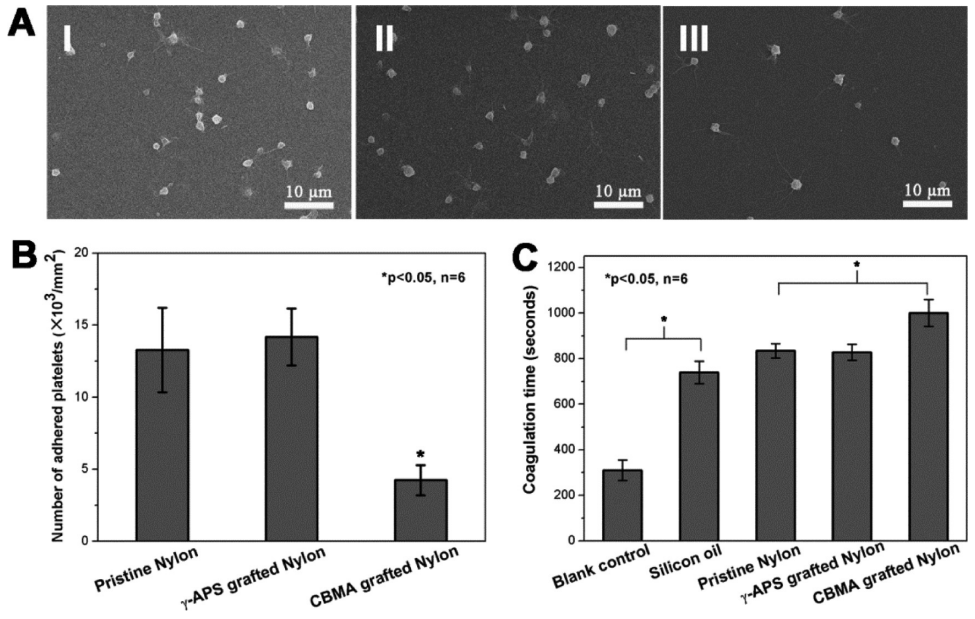

Figure 4. (A) Typical SEM photographs of the adhesion of platelets to pristine Nylon (I), γ-APS-grafted Nylon (II), and CBMA-grafted Nylon (III) surfaces. (B) Statistical number of adherent platelets. (C) Results of plasma recalcification time determination.

intensity and location can be found in N1s and O1s spectra. These changes are due to the coating of γ-APS and CBMA, which alter the amount of ammonium nitrogen and ester oxygen. In Si2p, an additional peak emerges in the γ-APS-modified Nylon spectrum, which clearly proves the successful graft of γ-APS, while in the CBMA-grafted Nylon Si2p spectrum, this peak becomes weak because of the covering of CBMA.

3.2. Blood Compatibility. *3.2.1. Wettability and BSA Adsorption.* The blood compatibility of the modified Nylon is of great importance given that the interaction of the Nylon surface with the blood constituent is vital for an interventional application.

The water contact angle (WCA) reveals the wettability of a material. Figure 3A shows the WCA of pristine and CBMA-grafted Nylon surfaces. The WCA of the Nylon surface decreased from 75.05 ± 0.77° to 50.07 ± 1.17° after CBMA grafting. As a result of the improvement in wettability, reduction of the adsorbed BSA on the sample surface was observed in all groups employing various BSA concentrations. As shown in Figure 3B, the amount of adsorbed BSA decreased from 94.32 ± 17.85 $\mu g/cm^2$ (1 mg/mL), 66.66 ± 10.56 $\mu g/cm^2$ (0.5 mg/mL), and 25.98 ± 6.54 $\mu g/cm^2$ (0.1 mg/mL) to 48.76 ± 7.79 $\mu g/cm^2$ ($p < 0.01$), 21.92 ± 7.80 $\mu g/cm^2$ ($p < 0.01$), and 8.14 ± 2.25 $\mu g/cm^2$ ($p < 0.01$), respectively.

Previous study indicated that the polar functional groups such as OH, NH_2, and COOH groups can enhance hydrogen bonding, thereby causing a decrease in the WCA of the surface.[42] Our results also show that the surface of CBMA-grafted Nylon possessed a wettability better than that of pristine Nylon (Figure 3A). It can be explained by the introduction of a COOH group onto the Nylon surface via CBMA grafting. Additionally, we found that the CBMA-grafted Nylon surface possessed a stronger ability to resist BSA adsorption (Figure 3B). It is widely known that proteins adhere to the surface of material in a nonspecific manner within a few seconds of water being absorbed by the material.[43] The adhesion of nonspecific proteins plays an important role in material-related coagulation.[44] Materials that are more hydrophilic can reduce the amount of nonspecific proteins absorbed on the surface because of the presence of a hydrated layer on the surface, which was caused by high-ratio free water.[45] Our results are consistent with the predictions prompted by these theories. In short, the hydrophility and the ability to resist

dx.doi.org/10.1021/am500394j | ACS Appl. Mater. Interfaces 2014, 6, 4550−4559

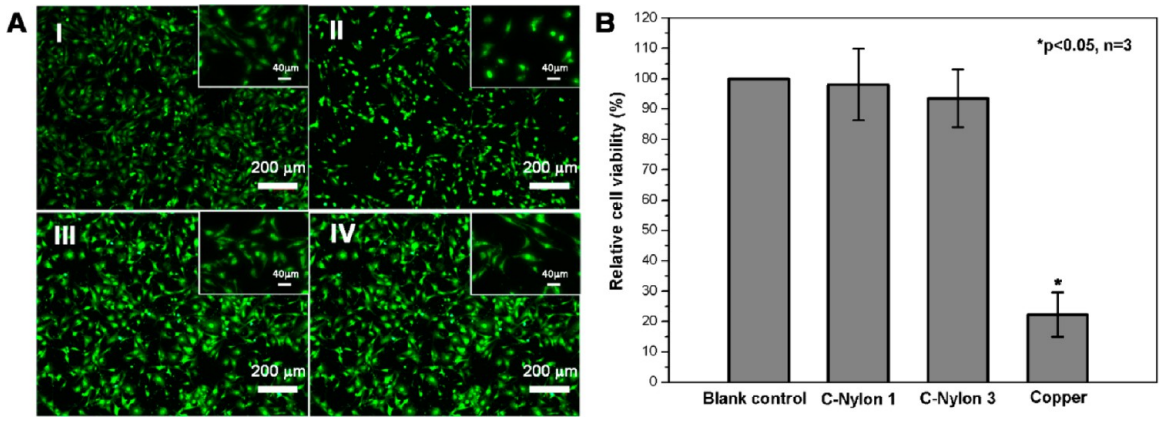

Figure 5. (A) Cytotoxic tests on HUVECs. Typical photographs of HUVECs after the tests: (I) cells cultured with an untreated ECM solution, (II) cells cultured with a copper-processed ECM solution, (III) cells cultured with 3 cm^2 of a CBMA-grafted Nylon-processed ECM solution, and (IV) cells cultured with 9 cm^2 of a CBMA-grafted Nylon-processed ECM solution. (B) Histogram of the viability of HUVECs after the tests. The scale bars in the main fluorescent images are 200 μm. The scale bars in the insets are 40 μm. Abbreviations: C-Nylon 1, low-concentration group of an ECM solution processed by CBMA-grafted Nylon; C-Nylon 3, high-concentration group of an ECM solution processed by CBMA-grafted Nylon.

protein absorption of the Nylon surface improved after CBMA had been grafted to it.

3.2.2. Anticoagulation Property. Figure 4 shows the results of coagulation experiments. Typical SEM photographs of adhesive platelets on a Nylon surface are shown in Figure 4A. Figure 4B shows the density of adhesive platelets by counting followed by unit conversion. The densities of adhesive platelets were $(1.33 \pm 0.29) \times 10^4$ cells/mm^2 for pristine Nylon, $(1.42 \pm 0.20) \times 10^4$ cells/mm^2 for γ-APS-grafted Nylon, and $(4.24 \pm 1.04) \times 10^3$ cells/mm^2 for CBMA-grafted Nylon. The difference between pristine Nylon and CBMA-grafted Nylon was significant ($p < 0.01$), as was the difference between γ-APS-grafted Nylon and CBMA-grafted Nylon ($p < 0.01$).

CBMA was grafted on Nylon by using γ-APS as the coupling reagent. The decrease in the density of adhesive platelets can be related to the introduction of γ-APS or CBMA. However, Franco et al. indicated that the amino group favors cell adhesion.[46] The work by Yoshioka et al. also revealed that γ-APS coating increases the level of platelet adhesion of the material surface.[39] In terms of our study, an increase in the mean value of adhered platelets could be observed on γ-APS-modified Nylon compared with that of pristine Nylon, while the difference was not statistically significant ($p = 0.545$). Hence, we proposed that the decrease in the level of platelet adhesion was a result of CBMA grafting. Zwitterionic betaine groups and hydrophilic groups of CBMA improved the wettability and subsequently minimized the interactions between platelets and the sample surface.

PRT is also an important indicator of the blood compatibility for the interventional material. In our investigation, a glass slide and a silicon oil-coated glass slide were used as a blank and positive control, respectively. Figure 4C shows the results of PRT determination. As the result of the decrease in the density of platelets and level of protein adhesion, the CBMA-grafted Nylon surface possessed the longest PRT (983.67 ± 36.95 s). All samples showed prolonged PRTs compared to that of the blank control ($p < 0.05$). The difference in PRT between pristine Nylon (834.17 ± 31.56 s) and CBMA-grafted Nylon (983.67 ± 36.95 s) was significant ($p < 0.01$), as well, while the difference between pristine Nylon (834.17 ± 31.56 s) and γ-APS-grafted Nylon (827.50.67 ± 35.46 s) was not ($p = 0.738$). We can conclude that better anticoagulation properties were obtained by grafting CBMA to Nylon.

3.3. Cytotoxicity Tests. To evaluate the biological safety of CBMA-grafted Nylon, we performed cytotoxicity tests.

An ECM culture solution was prepared as described in the Experimental Section. HUVECs were individually cultured using pristine Nylon and three ECM solutions that were prepared by different methods for 24 h before being observed with a microscope and subjected to viability test. Under a fluorescence microscope, a similar cell density and a normal adherent morphology could be found in the control group and two CBMA exposure groups (Figure 5A, I, III, and IV). In the copper exposure group, HUVECs lost their typical spindle shape and became spherical (Figure 5A, II). A decrease in cell density could also be found in this group (Figure 5A, II). Moreover, the CCK-8 kit was used to quantitatively test the viability of HUVECs. On the basis of the viability of the control group, the relative viability was calculated. The relative viabilities of two Nylon groups and the copper group were 98.1 ± 11.8% ($p = 0.793$), 93.6 ± 9.5% ($p = 0.362$), and 22.3 ± 7.3% ($p < 0.01$), respectively (Figure 5B).

As our device was designed for interventional use, potential injury to vascular endothelial cells must be avoided. HUVECs were widely used as a cell line surrogate for venous endothelial cells in previous studies.[47] The cytotoxicity of cooper ions, as heavy metal ions, has also been reported.[48] Therefore, in our study, using untreated ECM as a blank control and copper-treated ECM as a positive control, we performed this cytotoxicity test. Our results suggested that, unlike copper, a culture solution treated with CBMA-grafted Nylon had no negative influence on HUVECs. Our results showed that CBMA-grafted Nylon possessed no cytotoxicity and, therefore, could be safely used for the purpose of intervention.

3.4. Tumor Cell Adhesion. Our tumor cell adhesion experiments were performed to show the possibility of capturing CTCs using our modified and antibody-immobilized Nylon.

The epithelial cell adhesion molecule (EpCAM) is a 40 kDa monomeric membrane glycoprotein and is overexpressed in most carcinomas. EpCAM is widely used as target molecule in the existing CTC detection methods because of its expression deficiency in normal blood cells. However, the EpCAM

dx.doi.org/10.1021/am500394j | ACS Appl. Mater. Interfaces 2014, 6, 4550−4559

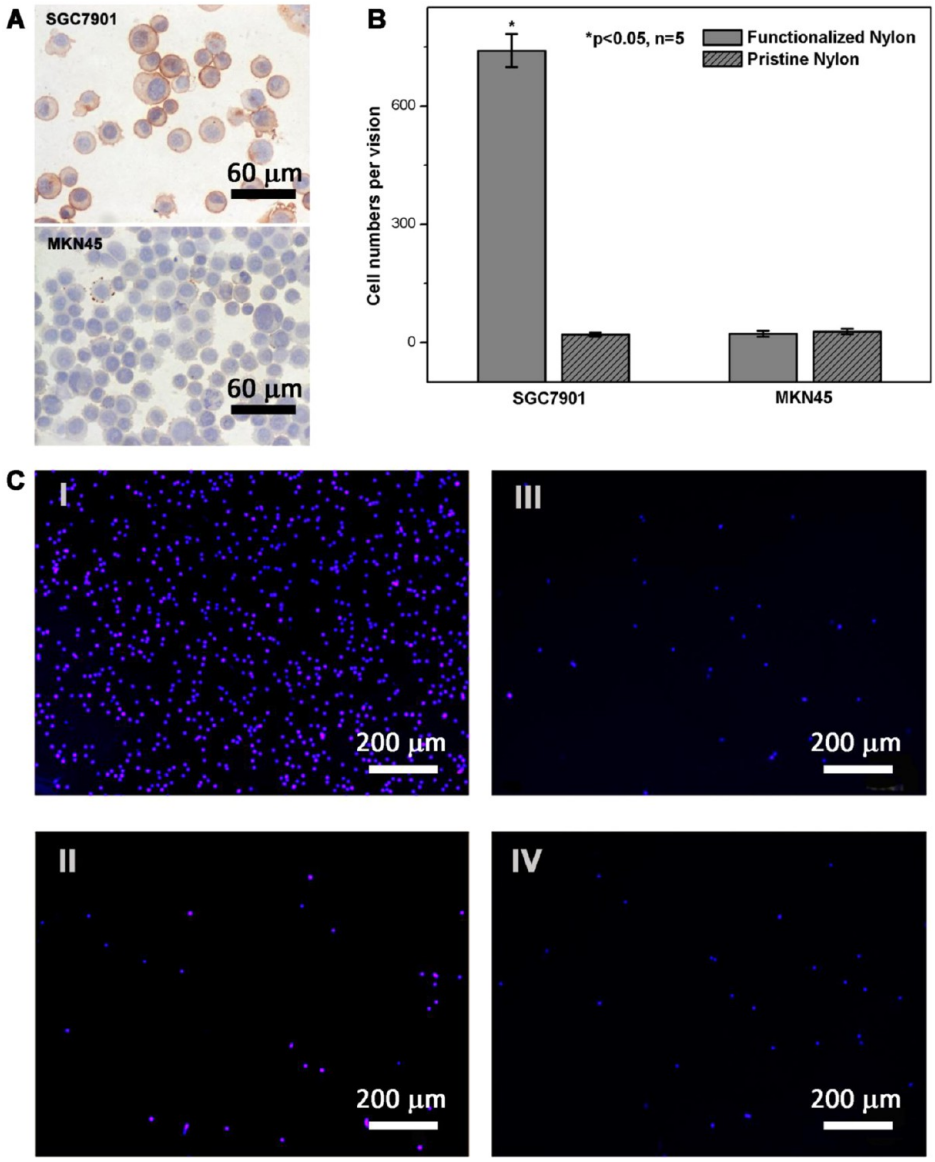

Figure 6. (A) Immunocytochemistry of MKN45 and SGC7901 cells. (B) Statistical number of adherent cells. (C) Typical photographs of adherent cells: (I) SGC7901 cells on functionalized and (II) pristine Nylon and (III) MKN45 cells on functionalized and (IV) pristine Nylon.

expression level of cancer cell lines was found to be variable.[49] Therefore, we investigated the EpCAM expression of four gastric cancer cell lines by immunocytochemistry before our tumor cell adhesion experiments.

As shown in Figure 6A, almost all cells of the SGC7901 cell line exhibited positive expression on a cell membrane while the MKN45 cell line exhibited the complete opposite. MKN28 and BGC823 cell lines showed partial expression of EpCAM (Figure S2, Supporting Information). Hence, the SGC7901 cell line was chosen for our cell adhesion experiment on functionalized Nylon, and the MKN45 cell line was used as a negative control.

The histogram in Figure 6B shows the results of tumor cell adhesion experiments. We found that the functionalized Nylon surface adhered to a vast number of SGC7901 tumor cells (740 ± 42 cells/vision), while few adhered to the pristine Nylon surface (20 ± 5 cells/vision) ($p < 0.01$). For the negative control (MKN45 cell line), very few tumor cells remained on the pristine (22 ± 8 cells/vision) or functionalized (28 ± 7 cells/vision) Nylon surface. Figure 6C shows typical photographs of various samples. Remarkably, the functionalized Nylon surface captured a larger amount of EpCAM positive tumor cells than the pristine Nylon surface. Our results revealed that good affinity for EpCAM positive tumor cells is obtained after the modification and antibody immobilization of Nylon. Though the anti-EpCAM antibody is the most widely used antibody for CTC capture, a new concept named "immunological cocktail" is becoming noteworthy.[50] The combination of EpCAM and other tumor specific antibodies or aptamers seems to be a promising way to improve CTC capture efficiency. For instance, ErbB2 (known as HER2) is specifically expressed in certain breast and gastric cancer cells. To the best of our knowledge, the anti-ErbB2 antibody has been used in the field of CTC capture.[51]

3.5. *In Vivo* CTC Capture Ability. We performed our *in vivo* CTC capture experiment to investigate the capture ability of the interventional device using a nude mouse tumor model.

dx.doi.org/10.1021/am500394j | ACS Appl. Mater. Interfaces 2014, 6, 4550−4559

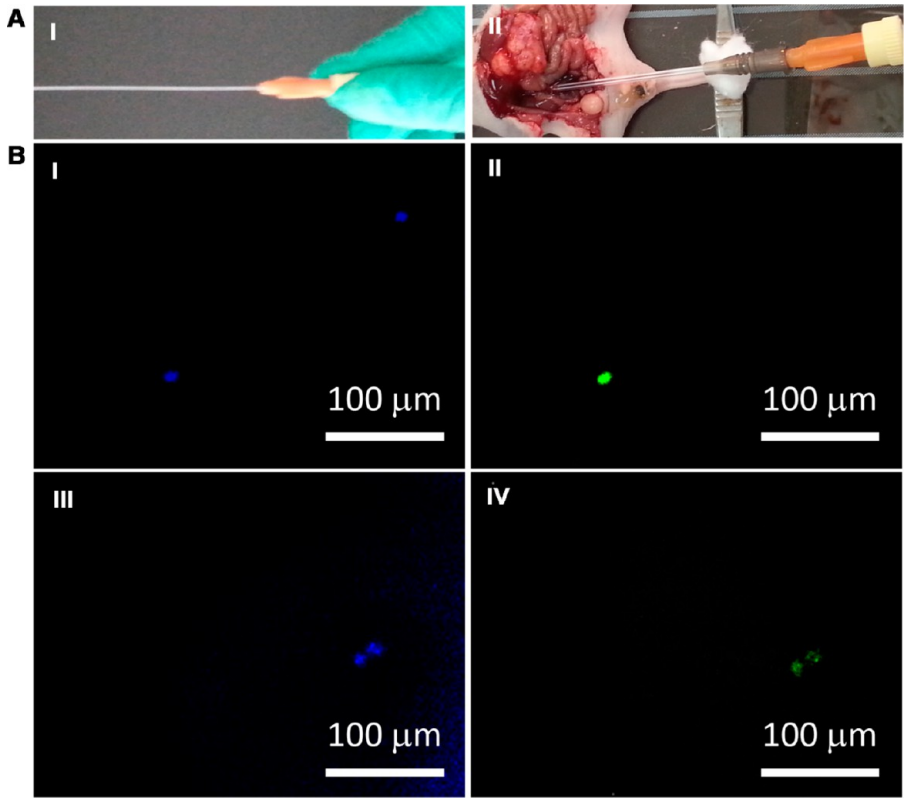

Figure 7. (A) Interventional device (I) and (II) scene of *in vivo* CTC capture on a nude mouse tumor model. (B) Typical fluorescent pictures of the wire surface after *in vivo* CTC capture and incubation of DAPI and the anti-pan Cytokeratin antibody. Images I and II show the same view of the surface under two different excitation lights, as do images III and IV.

The dissection of the postcava and the puncture of the trocar are shown in the Supporting Information.

Figure 7A shows the pictures of the interventional device (I) that was made of the modified Nylon wire and the scene after the insertion of that device (II). Thirty minutes after the device had been inserted, the wire was pulled out and further processed to visualize the cells on its surface.

Cytokeratin is a protein family that has more than 20 members. These proteins are expressed on human epithelial cells. Because cancer cells are epithelial cells and blood cells are not, the expression of Cytokeratin was widely used to distinguish CTCs from blood cells in recent studies focusing on CTC capture.[52] In our study, DAPI was used to assist in showing the cell nucleus and the FITC-labeled anti-pan Cytokeratin antibody in revealing CTCs. A total of three CTCs were captured by our device, and no CTCs were found on the unmodified Nylon wire. Representative pictures of the captured CTCs are shown in Figure 7B. In Figure 7B, images I and II show the same view under two different excitation lights, as do images III and IV. In image I of Figure 7B, two cells could be found. However, only one cell possessed Cytokeratin expression as shown in image II of Figure 7B. Therefore, we believed that the superficial cell was a residual blood cell and the inferior one was a CTC. In images III and IV of Figure 7B, two cells were both captured CTCs as dual positive fluorescent staining of DAPI and Cytokeratin could be observed.

The result of this experiment demonstrated the CTC capture ability of the interventional device in a nude mouse tumor model. We thought that the low concentration of CTCs and the small total blood volume of the mouse (2 mL) might partially explain why only three CTCs were captured. Because of the development of molecular biological techniques, studies focusing on testing genetic information on a single-CTC level revealed that even a single CTC could provide sufficient information for clinical management.[53,54] Therefore, this result of the *in vivo* capture showed the potential feasibility of the clinical use of our CTC capture device using modified Nylon in the future. However, several limitations of this *in vivo* experiment should be discussed. First, the 10 mm working length was chosen considering the anatomical structure of the nude mouse. As the postcava of the nude mouse is short, a Nylon wire that is longer than 10 mm could possibly stick into the right atrium, which would lead to the death of the mouse. Second, in our *in vivo* capture, the mouse must be kept alive to ensure the circulation of blood. After the laparotomy, almost the entire enterocoelia of the mouse was exposed. For this reason, it was difficult to keep the mouse alive for a period of time that was longer than 30 min. Hence, improvements in the device parameters such as working length, contact time, antibody selection, etc., are quite necessary for obtaining better CTC capture efficiency in potential human trials.

4. CONCLUSION

In our study, CBMA grafting and anti-EpCAM antibody immobilization on a Nylon surface were successfully performed as proven by ATR-FTIR, XPS, and cell adhesion experiments, serving the purpose of modifying Nylon as an appropriate material for the fabrication of interventional devices that can be used for *in vivo* CTC capture. The handled Nylon exhibited better biocompatibilities. Moreover, functionalized Nylon with our modification was shown to possess a better affinity for tumor cells expressing EpCAM. Most importantly, the CTC

capture ability of the interventional device created by our modified Nylon was demonstrated using a nude mouse tumor model. On the basis of our study, CBMA-grafted and anti-EpCAM antibody-immobilized Nylon is of great potential for use in the manufacture of interventional CTC capture devices, which are no longer limited by the volume of blood like traditional *in vitro* CTC detection methods. Moreover, the simple modification procedure employed in this study also makes it possible to further improve current interventional devices such as the introducer, the wire, the catheter, etc. The evolution of the CTC capture devices suggested by our study will provide oncologists with alternative approaches in the diagnosis of cancer. Furthermore, our novel *in vivo* CTC capture devices have the potential to move the concept of personalized cancer treatments one step closer to reality.

■ ASSOCIATED CONTENT

Ⓢ Supporting Information

Further details of the NMR spectrum (^{1}H) of CBMA, immunocytochemistry of BGC823 and MKN28 cells, and dissection of the postcava. This material is available free of charge via the Internet at http://pubs.acs.org.

■ AUTHOR INFORMATION

Corresponding Authors

*E-mail: baoruiliu@nju.edu.cn.
*E-mail: ztnj@nju.edu.cn.

Notes

The authors declare no competing financial interest.

■ ACKNOWLEDGMENTS

We acknowledge the support of the Projects of International Cooperation and Exchanges NSFC (81220108023), Jiangsu Province's Key Medical Center (BL2012001), the National Basic Research Program of China (2011CB933400), and the Science and Technology Support Program (Society Development) of Jiangsu Province (BE2012735). This work is also a part of the project funded by the Priority Academic Program Development of Jiangsu Higher Education Institutions (PAPD) and Jiangsu Province's Key Medical Center.

■ ABBREVIATIONS

CBMA, carboxybetaine methacrylate
CTCs, circulating tumor cells
EpCAM, epithelial cell adhesion molecule

■ REFERENCES

(1) Pantel, K.; Brakenhoff, R. H. Dissecting the metastatic cascade. *Nat. Rev. Cancer* **2004**, *4*, 448−456.
(2) Ma, X. L.; Xiao, Z. L.; Liu, L.; Liu, X. X.; Nie, W.; Li, P.; Chen, N. Y.; Wei, Y. Q. Meta-analysis of Circulating Tumor Cells as a Prognostic Marker in Lung Cancer. *Asian Pacific Journal of Cancer Prevention* **2012**, *13*, 1137−1144.
(3) Zhang, L.; Riethdorf, S.; Wu, G.; Wang, T.; Yang, K.; Peng, G.; Liu, J.; Pantel, K. Meta-analysis of the prognostic value of circulating tumor cells in breast cancer. *Clin. Cancer Res.* **2012**, *18*, 5701−5710.
(4) Zhao, S.; Liu, Y.; Zhang, Q.; Li, H.; Zhang, M.; Ma, W.; Zhao, W.; Wang, J.; Yang, M. The prognostic role of circulating tumor cells (CTCs) detected by RT-PCR in breast cancer: A meta-analysis of published literature. *Breast Cancer Res. Treat.* **2011**, *130*, 809−816.
(5) Zhang, L.; Wu, G.; Pantel, K. Detection of circulating tumor cells by RT-PCR significantly associated with poor prognosis in breast cancer. *Breast Cancer Res. Treat.* **2011**, *130*, 359−364.
(6) Rahbari, N. N.; Aigner, M.; Thorlund, K.; Mollberg, N.; Motschall, E.; Jensen, K.; Diener, M. K.; Buchler, M. W.; Koch, M.; Weitz, J. Meta-analysis shows that detection of circulating tumor cells indicates poor prognosis in patients with colorectal cancer. *Gastroenterology* **2010**, *138*, 1714−1726.
(7) Mocellin, S.; Hoon, D.; Ambrosi, A.; Nitti, D.; Rossi, C. R. The prognostic value of circulating tumor cells in patients with melanoma: A systematic review and meta-analysis. *Clin. Cancer Res.* **2006**, *12*, 4605−4613.
(8) Wang, F. B.; Yang, X. Q.; Yang, S.; Wang, B. C.; Feng, M. H.; Tu, J. C. A higher number of circulating tumor cells (CTC) in peripheral blood indicates poor prognosis in prostate cancer patients: A meta-analysis. *Asian Pacific Journal of Cancer Prevention* **2011**, *12*, 2629−2635.
(9) Alix-Panabieres, C.; Schwarzenbach, H.; Pantel, K. Circulating tumor cells and circulating tumor DNA. *Annu. Rev. Med.* **2012**, *63*, 199−215.
(10) Bossolasco, P.; Ricci, C.; Farina, G.; Soligo, D.; Pedretti, D.; Scanni, A.; Deliliers, G. L. Detection of micrometastatic cells in breast cancer by RT-pCR for the mammaglobin gene. *Cancer Detect. Prev.* **2002**, *26*, 60−63.
(11) Iakovlev, V. V.; Goswami, R. S.; Vecchiarelli, J.; Arneson, N. C.; Done, S. J. Quantitative detection of circulating epithelial cells by Q-RT-PCR. *Breast Cancer Res. Treat.* **2008**, *107*, 145−154.
(12) Xenidis, N.; Perraki, M.; Kafousi, M.; Apostolaki, S.; Bolonaki, I.; Stathopoulou, A.; Kalbakis, K.; Androulakis, N.; Kouroussis, C.; Pallis, T.; Christophylakis, C.; Argyraki, K.; Lianidou, E. S.; Stathopoulos, S.; Georgoulias, V.; Mavroudis, D. Predictive and prognostic value of peripheral blood cytokeratin-19 mRNA-positive cells detected by real-time polymerase chain reaction in node-negative breast cancer patients. *J. Clin. Oncol.* **2006**, *24*, 3756−3762.
(13) Cabioglu, N.; Igci, A.; Yildirim, E. O.; Aktas, E.; Bilgic, S.; Yavuz, E.; Muslumanoglu, M.; Bozfakioglu, Y.; Kecer, M.; Ozmen, V.; Deniz, G. An ultrasensitive tumor enriched flow-cytometric assay for detection of isolated tumor cells in bone marrow of patients with breast cancer. *Am. J. Surg.* **2002**, *184*, 414−417.
(14) Cruz, I.; Ciudad, J.; Cruz, J. J.; Ramos, M.; Gomez-Alonso, A.; Adansa, J. C.; Rodriguez, C.; Orfao, A. Evaluation of multiparameter flow cytometry for the detection of breast cancer tumor cells in blood samples. *Am. J. Clin. Pathol.* **2005**, *123*, 66−74.
(15) Simpson, S. J.; Vachula, M.; Kennedy, M. J.; Kaizer, H.; Coon, J. S.; Ghalie, R.; Williams, S.; Van Epps, D. Detection of tumor cells in the bone marrow, peripheral blood, and apheresis products of breast cancer patients using flow cytometry. *Exp. Hematol.* **1995**, *23*, 1062−1068.
(16) Braun, S.; Vogl, F. D.; Naume, B.; Janni, W.; Osborne, M. P.; Coombes, R. C.; Schlimok, G.; Diel, I. J.; Gerber, B.; Gebauer, G.; Pierga, J. Y.; Marth, C.; Oruzio, D.; Wiedswang, G.; Solomayer, E. F.; Kundt, G.; Strobl, B.; Fehm, T.; Wong, G. Y.; Bliss, J.; Vincent-Salomon, A.; Pantel, K. A pooled analysis of bone marrow micrometastasis in breast cancer. *N. Engl. J. Med.* **2005**, *353*, 793−802.
(17) Pachmann, K.; Camara, O.; Kavallaris, A.; Krauspe, S.; Malarski, N.; Gajda, M.; Kroll, T.; Jorke, C.; Hammer, U.; Altendorf-Hofmann, A.; Rabenstein, C.; Pachmann, U.; Runnebaum, I.; Hoffken, K. Monitoring the response of circulating epithelial tumor cells to adjuvant chemotherapy in breast cancer allows detection of patients at risk of early relapse. *J. Clin. Oncol.* **2008**, *26*, 1208−1215.
(18) Ring, A. E.; Zabaglo, L.; Ormerod, M. G.; Smith, I. E.; Dowsett, M. Detection of circulating epithelial cells in the blood of patients with breast cancer: Comparison of three techniques. *Br. J. Cancer* **2005**, *92*, 906−912.
(19) Zabaglo, L.; Ormerod, M. G.; Parton, M.; Ring, A.; Smith, I. E.; Dowsett, M. Cell filtration-laser scanning cytometry for the characterisation of circulating breast cancer cells. *Cytometry, Part A* **2003**, *55*, 102−108.
(20) Cristofanilli, M.; Budd, G. T.; Ellis, M. J.; Stopeck, A.; Matera, J.; Miller, M. C.; Reuben, J. M.; Doyle, G. V.; Allard, W. J.; Terstappen, L. W.; Hayes, D. F. Circulating tumor cells, disease progression, and

survival in metastatic breast cancer. *N. Engl. J. Med.* **2004**, *351*, 781−791.
(21) Riethdorf, S.; Fritsche, H.; Muller, V.; Rau, T.; Schindlbeck, C.; Rack, B.; Janni, W.; Coith, C.; Beck, K.; Janicke, F.; Jackson, S.; Gornet, T.; Cristofanilli, M.; Pantel, K. Detection of circulating tumor cells in peripheral blood of patients with metastatic breast cancer: A validation study of the CellSearch system. *Clin. Cancer Res.* **2007**, *13*, 920−928.
(22) Nagrath, S.; Sequist, L. V.; Maheswaran, S.; Bell, D. W.; Irimia, D.; Ulkus, L.; Smith, M. R.; Kwak, E. L.; Digumarthy, S.; Muzikansky, A.; Ryan, P.; Balis, U. J.; Tompkins, R. G.; Haber, D. A.; Toner, M. Isolation of rare circulating tumour cells in cancer patients by microchip technology. *Nature* **2007**, *450*, 1235−1239.
(23) Wang, Y.; Zhou, F.; Liu, X.; Yuan, L.; Li, D.; Wang, Y.; Chen, H. Aptamer-modified micro/nanostructured surfaces: Efficient capture of Ramos cells in serum environment. *ACS Appl. Mater. Interfaces* **2013**, *5*, 3816−3823.
(24) Wu, C. H.; Huang, Y. Y.; Chen, P.; Hoshino, K.; Liu, H.; Frenkel, E. P.; Zhang, J. X.; Sokolov, K. V. Versatile immunomagnetic nanocarrier platform for capturing cancer cells. *ACS Nano* **2013**, *7*, 8816−8823.
(25) Horák, D.; Svobodová, Z.; Autebert, J.; Coudert, B.; Plichta, Z.; Královec, K.; Bílková, Z.; Viovy, J. L. Albumin-coated monodisperse magnetic poly(glycidyl methacrylate) microspheres with immobilized antibodies: Application to the capture of epithelial cancer cells. *J. Biomed. Mater. Res., Part A* **2013**, *101*, 23−32.
(26) Hou, S.; Zhao, H.; Zhao, L.; Shen, Q.; Wei, K. S.; Suh, D. Y.; Nakao, A.; Garcia, M. A.; Song, M.; Lee, T.; Xiong, B.; Luo, S. C.; Tseng, H. R.; Yu, H. H. Capture and stimulated release of circulating tumor cells on polymer-grafted silicon nanostructures. *Adv. Mater.* **2013**, *25*, 1547−1551.
(27) Shen, Q.; Xu, L.; Zhao, L.; Wu, D.; Fan, Y.; Zhou, Y.; Ouyang, W. H.; Xu, X.; Zhang, Z.; Song, M.; Lee, T.; Garcia, M. A.; Xiong, B.; Hou, S.; Tseng, H. R.; Fang, X. Specific capture and release of circulating tumor cells using aptamer-modified nanosubstrates. *Adv. Mater.* **2013**, *25*, 2368−2373.
(28) Gorges, T. M.; Pantel, K. Circulating tumor cells as therapy-related biomarkers in cancer patients. *Cancer Immunol. Immunother.* **2013**, *62*, 931−939.
(29) Chegini, N.; von Fraunhofer, J. A.; Hay, D. L.; Stone, I. K.; Masterson, B. J. The use of nylon pouches to prevent cellular attachment to implanted materials. *Biomaterials* **1987**, *8*, 315−319.
(30) Beeskow, T.; Kroner, K. H.; Anspach, F. B. Nylon-Based Affinity Membranes: Impacts of Surface Modification on Protein Adsorption. *J. Colloid Interface Sci.* **1997**, *196*, 278−291.
(31) Nuhiji, E.; Wong, C. S.; Sutti, A.; Lin, T.; Kirkland, M.; Wang, X. Biofunctionalization of 3D Nylon 6,6 Scaffolds Using a Two-Step Surface Modification. *ACS Appl. Mater. Interfaces* **2012**, *4*, 2912−2919.
(32) Yancey, P. H.; Clark, M. E.; Hand, S. C.; Bowlus, R. D.; Somero, G. N. Living with water stress: Evolution of osmolyte systems. *Science* **1982**, *217*, 1214−1222.
(33) Kitano, H.; Tada, S.; Mori, T.; Takaha, K.; Gemmei-Ide, M.; Tanaka, M.; Fukuda, M.; Yokoyama, Y. Correlation between the structure of water in the vicinity of carboxybetaine polymers and their blood-compatibility. *Langmuir* **2005**, *21*, 11932−11940.
(34) Zhou, J.; Yuan, J.; Zang, X.; Shen, J.; Lin, S. Platelet adhesion and protein adsorption on silicone rubber surface by ozone-induced grafted polymerization with carboxybetaine monomer. *Colloids Surf., B* **2005**, *41*, 55−62.
(35) Zhang, Z.; Chao, T.; Chen, S.; Jiang, S. Superlow fouling sulfobetaine and carboxybetaine polymers on glass slides. *Langmuir* **2006**, *22*, 10072−10077.
(36) Ladd, J.; Zhang, Z.; Chen, S.; Hower, J. C.; Jiang, S. Zwitterionic polymers exhibiting high resistance to nonspecific protein adsorption from human serum and plasma. *Biomacromolecules* **2008**, *9*, 1357−1361.
(37) Liaw, D. J.; Huang, C. C.; Lee, W. F.; Borbely, J.; Kang, E. T. Synthesis and characteristics of the poly(carboxybetaine)s and the corresponding cationic polymers. *J. Polym. Sci., Part A: Polym. Chem.* **1997**, *35*, 3527−3536.
(38) Zhang, Z. B.; Zhu, X. L.; Xu, F. J.; Neoh, K. G.; Kang, E. T. Temperature- and pH-sensitive nylon membranes prepared via consecutive surface-initiated atom transfer radical graft polymerizations. *J. Membr. Sci.* **2009**, *342*, 300−306.
(39) Yoshioka, T.; Tsuru, K.; Hayakawa, S.; Osaka, A. Preparation of alginic acid layers on stainless-steel substrates for biomedical applications. *Biomaterials* **2003**, *24*, 2889−2894.
(40) Russell, R. J.; Sirkar, K.; Pishko, M. V. Preparation of nanocomposite poly(allylamine)-poly(ethylene glycol) thin films using Michael addition. *Langmuir* **2000**, *16*, 4052−4054.
(41) Zhang, Z.; Chen, S.; Jiang, S. Dual-functional biomimetic materials: Nonfouling poly(carboxybetaine) with active functional groups for protein immobilization. *Biomacromolecules* **2006**, *7*, 3311−3315.
(42) Teasdale, P. R.; Wallace, G. G. In situ characterization of conducting polymers by measuring dynamic contact angles with Wilhelmy's plate technique. *React. Funct. Polym.* **1995**, *24*, 157−164.
(43) Xu, Y.; Dong, A.; Zhao, Y.; Zhang, T.; Jiang, Z.; Wang, S.; Chen, H. Synthesis, Characterization and Biomedical Properties of UV-Cured Polyurethane Acrylates Containing a Phosphorylcholine Structure. *J. Biomater. Sci., Polym. Ed.* **2012**, *23*, 2089−2104.
(44) Li, X.; Luan, S.; Yuan, S.; Song, L.; Zhao, J.; Ma, J.; Shi, H.; Yang, H.; Jin, J.; Yin, J. Surface functionalization of styrenic block copolymer elastomeric biomaterials with hyaluronic acid via a "grafting to" strategy. *Colloids Surf., B* **2013**, *112*, 146−154.
(45) Ishihara, K.; Nomura, H.; Mihara, T.; Kurita, K.; Iwasaki, Y.; Nakabayashi, N. Why do phospholipid polymers reduce protein adsorption? *J. Biomed. Mater. Res.* **1998**, *39*, 323−330.
(46) Franco, M.; Nealey, P. F.; Campbell, S.; Teixeira, A. I.; Murphy, C. J. Adhesion and proliferation of corneal epithelial cells on self-assembled monolayers. *J. Biomed. Mater. Res.* **2000**, *52*, 261−269.
(47) Tong, H.; Wan, P.; Zhang, X.; Duan, P.; Tang, Y.; Chen, Y.; Tang, L.; Su, L. Vascular endothelial cell injury partly induced by mesenteric lymph in heat stroke. *Inflammation* **2014**, *37*, 27−34.
(48) Thit, A.; Selck, H.; Bjerregaard, H. F. Toxicity of CuO nanoparticles and Cu ions to tight epithelial cells from *Xenopus laevis* (A6): Effects on proliferation, cell cycle progression and cell death. *Toxicol. In Vitro* **2013**, *27*, 1596−1601.
(49) Sterzynska, K.; Kempisty, B.; Zawierucha, P.; Zabel, M. Analysis of the specificity and selectivity of anti-EpCAM antibodies in breast cancer cell lines. *Folia Histochem. Cytobiol.* **2012**, *50*, 534−541.
(50) Uhr, J. W. The clinical potential of circulating tumor cells; the need to incorporate a modern "immunological cocktail" in the assay. *Cancers* **2013**, *5*, 1739−1747.
(51) Galletti, G.; Sung, M. S.; Vahdat, L. T.; Shah, M. A.; Santana, S. M.; Altavilla, G.; Kirby, B. J.; Giannakakou, P. Isolation of breast cancer and gastric cancer circulating tumor cells by use of an anti HER2-based microfluidic device. *Lab Chip* **2014**, *14*, 147−156.
(52) Josse, S. A.; Pantel, K. Biologic challenges in the detection of circulating tumor cells. *Cancer Res.* **2013**, *73*, 8−11.
(53) Powell, A. A.; Talasaz, A. H.; Zhang, H.; Coram, M. A.; Reddy, A.; Deng, G.; Telli, M. L.; Advani, R. H.; Carlson, R. W.; Mollick, J. A.; Sheth, S.; Kurian, A. W.; Ford, J. M.; Stockdale, F. E.; Quake, S. R.; Pease, R. F.; Mindrinos, M. N.; Bhanot, G.; Dairkee, S. H.; Davis, R. W.; Jeffrey, S. S. Single cell profiling of circulating tumor cells: Transcriptional heterogeneity and diversity from breast cancer cell lines. *PLoS One* **2012**, e33788.
(54) Sakaizawa, K.; Goto, Y.; Kiniwa, Y.; Uchiyama, A.; Harada, K.; Shimada, S.; Saida, T.; Ferrone, S.; Takata, M.; Uhara, H.; Okuyama, R. Mutation analysis of BRAF and KIT in circulating melanoma cells at the single cell level. *Br. J. Cancer* **2012**, *106*, 939−946.